Charge-Transfer in Panchromatic Porphyrin-Tetracyanobuta-1,3-diene-Donor Conjugates: Switching the Role of Porphyrin in the Charge Separation Process

Bijesh Sekaran,^{[a],‡} Andrew Dawson,^{[b]‡} Youngwoo Jang,^[b] Kusum V. MohanSingh,^[a] Rajneesh Misra^{[a]*} and Francis D'Souza^{[b]*}

Abstract: Using a combination of cycloaddition-retroelectrocyclization reaction, free-base and zinc porphyrins (H_2P and ZnP) are decorated at their β-pyrrole positions with strong charge transfer complexes, viz., tetracyanobuta-1,3-diene (TCBD)-phenothiazine (3 and 4) or TCBD-aniline (7 and 8), novel class of push-pull systems. The physico-chemical properties of these compounds (MP-Donor and MP-TCBD-Donor) have been investigated using a range of electrochemical, spectroelectrochemical, DFT as well as steady-state and time-resolved spectroscopic techniques. Ground-state charge transfer interactions between the porphyrin and the electron-withdrawing TCBD directly attached to the porphyrin π-system extended the absorption features well into the near-infrared region. To visualize the photo-events, energy level diagrams with the help of free-energy calculations have been established. Switching the role of porphyrin from the initial electron acceptor to electron donor was possible to envision. Occurrence of photoinduced charge separation has been established by complementary transient absorption spectral studies followed by global and target data analyses. Better charge stabilization in H_2P derived over ZnP derived conjugates, and in phenothiazine derived over aniline derived conjugates has been possible to establish. These findings highlight the importance of the nature of porphyrins and second electron donor in governing the ground and excited state charge transfer events in closely positioned donor-acceptor conjugates.

Introduction

Photoinduced electron transfer (PET) is the main step in the conversion of solar light into chemical energy in plant and bacterial systems, [1-2] and a process with countless relevance in research fields including artificial photosynthesis, photocatalysis, photoconductivity, or molecular photovoltaics. [3-16] In a simplistic scheme, PET consists of two main steps, namely, light absorption

by a chromophore resulting in the formation of an excited state species, followed by a charge transfer between an electron donor (D) and an electron acceptor (A) leading to a charge separated D.+-A.- species.^[16] The optimization of these processes and comprehending their mutual interplay to ultimately achieving charge separated species is of paramount importance for the development of efficient systems in solar light conversion schemes.

Among the building blocks employed in the construction of light-active donor-acceptor conjugates, the large $\pi\text{-structured}$ porphyrins (P)[17-20] and phthalocyanines (Pc)[21-24] have occupied privileged position due to their structural resemblance to natural chlorophyll and bacteriochlorophyll found in green plants and bacteria, relative ease of chemical synthesis and

post functionalization, high fluorescence quantum yields, rich redox properties and good photo- and thermal stability. To-date, several P and Pc based architectures have been prepared, in which the macrocycles have been connected to electron donor and/or acceptor entities by either covalent or non-covalent methods. [3-24] In most of the D-A assemblies derived from P and Pc, photophysical studies in solution have demonstrated occurrence of intramolecular photoinduced electron transfer leading to solvent stabilized radical-ion pairs.

Figure 1. Structure of the newly synthesized and investigated MP-Donor and MP-TCBD-Donor (MP = 2H or Zn, Donor = PTZ or NND) conjugates, and the control compounds.

As part of our systematic investigation on the synthesis and study of novel porphyrin-based D-A systems capable of revealing ultrafast electron transfer,^[5,19,23] in the present study, we have utilized 1,1,4,4, -tetracyanobuta-1,3-diene (TCBD) as a partner for the porphyrin. TCBD is a cyano-rich moiety^[25] that has been covalently linked to many electroactive units including porphyrins, phthalocyanines and BODIPYs.^[26-45] In most of these TCBD-based D-A conjugates, photoinduced charge separation has been

 [[]a] B. Sekaran, K. V. MohanSingh, Prof. Dr. R. Misra Department of Chemistry, Indian Institute of Technology, Indore 453552, India. E-mail: rajneeshmisra@iiti.ac.in

[[]b] A. Dawson, Y. Jang, Prof. Dr. F. D'Souza Department of Chemistry, University of North Texas, 1155 Union Circle, #305070, Denton, TX 76203-5017, USA, E-mail: Francis.DSouza@UNT.edu

[‡] Equal contribution

Supporting information for this article, experimental and synthetic details, ¹H and ¹³C NMR and HRMS of synthesized compounds. Additional cyclic voltammetric, spectroelectrochemical, computational coordinates, and transient absorption spectral spectra.

observed as a consequence of coupling between the electronpoor TCBD and electron-rich sensitizer. In the literature reported porphyrin-TCBD systems,[41-42] porphyrin was functionalized at the meso-position with a TCBD entity either directly or with a phenyl ring spacer. Knowing the lack of directly linked porphyrin-TCBD conjugates utilizing the β -pyrrole positions and how that would modulate the electron transfer properties, in the present study, we have newly designed and synthesized porphyrin-TCBD conjugates, 3-4 and 7-8 as shown in Figure 1. Both free-base (H₂P, compounds 3 and 7) and its zinc(II) porphyrin (ZnP, compounds 4 and 8) derivatives have been utilized as they differ in their oxidation potentials modulating the free-energy change for charge separation (ZnPs are easier to oxidize by about 270 mV compared to H₂Ps), and have also utilized additional electron donors, phenothiazine (PTZ, compounds 3 and 4) and N,Ndimethylaniline (NND, compounds 7 and 8) to stabilize the TCBD entity in these D-A conjugates. Different degrees of TCBD-PTZ and TCBD-NND interactions is expected to modulate the reduction potentials of TCBD in this series of strong push-pull

Results and Discussion

Synthesis

Scheme 1. Synthetic routes developed for β -pyrrole functionalized push-pull porphyrins, **1–8**.

The synthetic routes for β -donor substituted TCBD functionalized push-pull porphyrins are shown in Scheme 1. The β -monobrominated tetraphenylporphyrin (TPPBr), **11** and the control compounds, **9** and **10** were synthesized according to the reported procedures (Figure 1 and Scheme 1). [46-48] The Pdcatalyzed Sonogashira cross-coupling reaction of TPPBr, **11** using one equiv of 3-ethynyl-10-propyl-10H-phenothiazine, **12** and 4-ethynyl-N, N-dimethylaniline, **13** in the presence of Pd(PPh₃)₄ in THF at 70 °C resulted in porphyrins **1** and **5** in 73 and 69% yields, respectively (Scheme 1). The zinc complexation of the porphyrins **1** and **5** was subsequently carried out using

Zn(OAc)₂ by dissolving in MeOH and CHCl₃ (3:1) mixture, which resulted in zinc derivatives, **2** and **6** in 86 and 83% yields, respectively. The TCBD functionalized push-pull porphyrins, **3**, **4**, and **7**, **8** were synthesized *via* [2 + 2] cycloaddition-retroelectrocyclization reaction and are shown in Scheme 1. The reaction of porphyrin and its zinc derivatives, **1**, **2**, **5** and **6** with TCNE, **14** in dichloroethane (DCE) resulted in β -substituted TCBD functionalized push-pull porphyrins, **3**, **4**, **7** and **8** in 91, 88, 91 and 91% yields, respectively. The porphyrin derivatives, **1**–**8** were fully characterized by ¹H and ¹³C NMR, HR-MS and MALDITOF mass spectra. (see supporting information for spectral details, Figures S9-S31).

Optical absorption and emission studies

The absorption spectra of β -pyrrole TCBD functionalized push-pull porphyrins and corresponding control compounds were recorded in benzonitrile at room temperature, and data are summarized in Table 1. The porphyrins exhibited a characteristic Soret band in the 425–440 nm region, and two to four Q-bands in the 510–670 nm region. Figures 2a and 2b illustrate the absorption spectra of phenothiazine and N, N-dimethylaniline derivatized zinc porphyrins while Figures S1a and S1b show those of the corresponding free-base porphyrin derivatives. The free-base porphyrins, $\bf 1$ and $\bf 5$ showed a Soret band and four Q

bands, whereas the Zn(II) porphyrins, 2 and 6 exhibited the characteristic Soret band and two Q bands in the visible region. Introducing TCBD at the β -pyrrole position of both free-base and zinc porphyrins resulted in bathochromic shift of about 10 nm of both Soret and visible bands suggesting electronic interaction between the entities. Importantly, in the near-IR region covering the 650-900 nm range, a new absorption band was observed in all TCBD bearing systems as a consequence of intramolecular charge

transfer involving the electron deficient TCBD and the electron rich porphyrin and second donor entities. $^{[33-43]}$ In summary, intramolecular charge transfer in the ground state was successfully established in these MP-TCBD-Donor (M = 2H or Zn; donor = PTZ or NND) conjugates.

Both steady-state and time-resolved fluorescence spectral studies of the investigated compounds was performed in benzonitrile. Figures 2c and 2d show the fluorescence spectra of zinc porphyrins, **2**, **4**, **6** and **8** while the free-base analogs are shown in Figure S1c and S1d. The β -donor substituted porphyrins showed the characteristic two emission bands in the low energy region. The free-base porphyrins, **1** and **5** showed emission in the

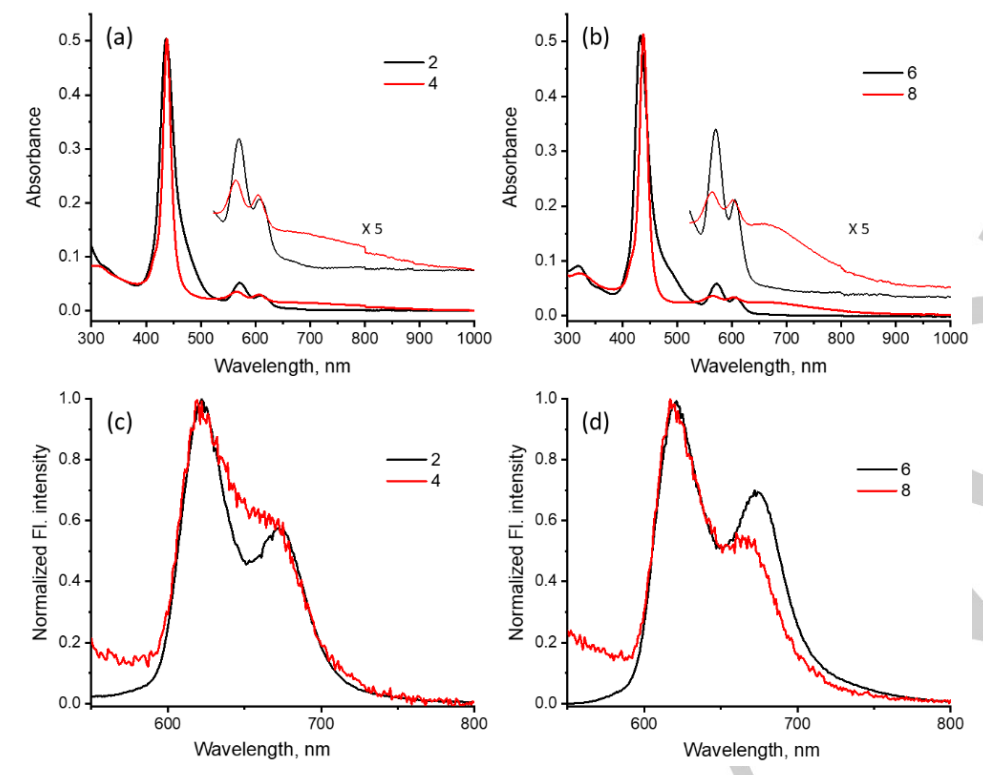


Figure 2. Normalized to the Soret band, absorption spectra of compounds (a) 2 and 4, and (b) 6 and 8 in benzonitrile. Fluorescence spectra, normalized to the 0,0 emission peak of compounds (c) 2 and 4, and (d) 6 and 8 in benzonitrile. The samples were excited to the Soret peak maxima.

650–740 nm range while their Zn(II) complexes, **2** and **6** revealed emission in the 600–670 nm range. Florescence intensity in both PTZ and NND bearing porphyrins was found to be quenched over 50-80% when compared to the control porphyrins, **9** and **10**, both having a phenyl ring instead of the electron donor. These results suggest occurrence of excited state events from the 1 MP* in MP-Donor (M = 2H or Zn; donor = PTZ or NND) dyads. Interestingly, in the case of MP-TCBD-Donor conjugates, such quenching was found to be even more pronounced, that is, quenching over 98%

was observed. The normalized fluorescence spectra shown in Figures 2c and d, and Figure S1c and d also revealed a small blueshift of the 0,1 peak, however, without the appearance of any new peak characteristic of charge transfer emission. It is likely that intensity of such transitions is rather low.

The lifetimes measured using correlated single photon counting (TCSPC) using nanoLED excitation sources also revealed such a trend. The lifetime of control porphyrins, 9 and 10 was found to be 8.73 and 1.78 ns, respectively, close to that expected for the freebase and zinc tetraphenylporphyrins. However. these lifetimes were found to be substantially quenched in MP-Donor dyads (see Table 1), a trend consistent with the steady-state fluorescence properties. In the case

of MP-TCBD-Donor conjugates, due to very weak emission, the lifetime was within the time resolution of our instrumental setup (~200 ps). These results indicate excited state events in both MP-Donor and MP-TCBD-Donor conjugates investigated here.

Visualizing excited state events through energy calculations

Fluorescence quenching observed in both MP-Donor and MP-TCBD-Donor conjugates suggest excited state events such as energy or electron transfer from singlet excited MP. Free-energy calculations based on spectral, electrochemical and geometry parameters help us in establishing energy level diagrams to visualize possible photo-excited events. With this in mind, first, electrochemical studies were performed using both

 Table 1. Absorption and fluorescence spectral data of the investigated compounds in benzonitrile.

Compound	λ_{abs} , nm	λ_{em} , nm	$\Phi_{f}^{[53]}$	τ _F , ns
1	427, 527, 566, 602, 658	662, 731	0.0169	3.18
2	437, 571, 609	622, 673	0.0139	1.40
3	429, 520, 551	663, 725	0.0010	
4	438, 566, 606	621, 671	0.0003	
5	424, 525, 570, 602	663, 729	0.0079	1.93
6	433, 572, 607	621, 674	0.0189	1.37
7	430, 522, 658	661, 725	0.0006	
8	439, 564, 604	618, 668	0.0004	
9	430, 520, 561, 600, 658	664, 727	0.0431	8.73
10	440, 566, 607	620, 670	0.0131	1.78

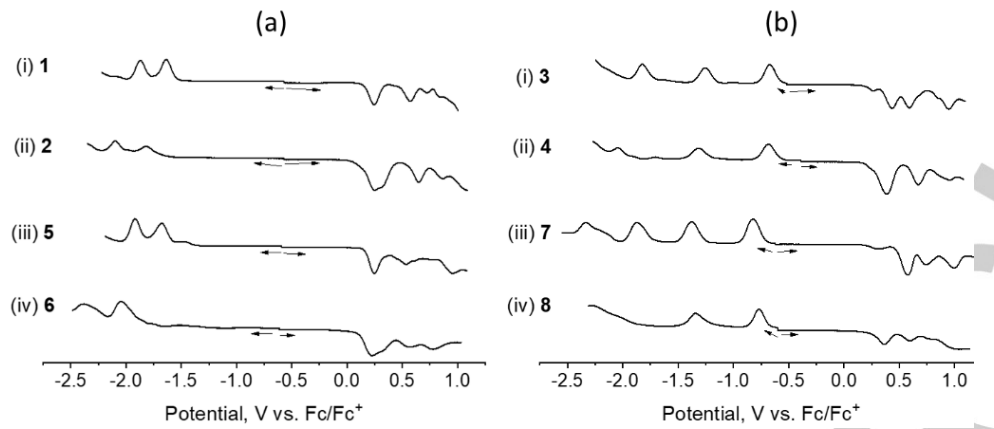


Figure 3. DPVs of the indicated compounds in benzonitrile containing 0.1 M n-Bu₄NClO₄. Scan rate = 5 mV/s, pulse width = 0.25 s, pulse height = 0.025 V. The potentials were referenced against internal ferrocene/ferrocenium redox couple.

differential pulse (DPV) and cyclic voltammetric (CV) techniques. DPVs of MP-Donor and MP-TCBD-Donor conjugates are shown in Figure 3 while the corresponding CVs are shown in Figure S2. Redox potentials are tabulated in Table 2. It is well known that both H_2P and ZnP reveal two one-electron oxidations and two one-electron reductions. [19] This is also the case for the control compounds **9** and **10**. The corresponding redox potentials of **9** were located at -1.86, -1.58, 0.47 and 0.72 V vs. Fc/Fc+ while that of **10** were located at -1.90, -1.79, 0.30 and 0.62 V. Easier oxidation of ZnP over H_2P for the β -pyrrole functionalized porphyrins was clear from this data. Having additional redox-

active entities linked to the porphyrin macrocycle is expected show additional oxidation and reduction peaks.[19] This seems to be the case in the present investigated series of compounds. As shown in Figure 3a, for the MP-Donor systems having a second donor entity (PTZ and NND), additional oxidations observed. In the case of 1 and 2 having a PTZ, and 5 and 6 having NND entities, the first oxidation was easier than that expected for the corresponding porphyrin

derivatives indicating that it involves oxidation of the second electron donor entity. The potentials for second oxidation process were close to that expected for MP suggesting it involves formation of MP/MP.* process (see Table 2). Introducing electrodeficient TCBD in MP-TCBD-Donor systems (3, 4, 7 and 8) revealed two additional reductions as shown in Figure 3b corresponding to TCBD^{0/.-} and TCBD^{-./2-} processes. In the case of 3 and 4, these processes were easier by nearly 120 mV compared to those in 7 and 8 revealing subtle influence of second electron donor. Additionally, presence of TCBD in MP-TCBD-Donor systems, induced cathodic shift of MP centered reductions by about 200 mV, and anodic shift of both Donor and MP centered oxidations by about 150-280 mV. These results unequivocally prove existence of intramolecular interactions involving TCBD and MP/Donor entities.

Table 2. Redox potentials and free-energy change for charge separation and recombination for the investigated compounds in benzonitrile.

Potential V vs. Fc/Fc ⁺													
Compound		Е	red			E	ox	7	E _{o,o} , eV	$E_{\rm CT}$, eV	$\Delta G_{\rm sol}$, eV	$-\Delta G_{\rm CS}$, eV	– $\Delta G_{\rm CR},{\rm eV}$
	MP	MP	TCBD	TCBD	MP-D	MP-D	MP-D	MP-D					
1	-1.87	-1.64		7	0.20	0.57	0.73	0.84	1.89		-0.205	0.21	1.68
2	-2.11	-1.82			0.25	0.32	0.65	0.86	2.04		-0.205	0.17	1.87
3		-1.83	-1.25	-0.67	0.43	0.59	0.95		2.10	1.11	-0.285	1.28	0.82
4		-2.04	-1.32	-0.69	0.38	0.67	0.95		2.09	1.07	-0.285	1.30	0.78
5	-1.92	-1.68		-	0.25	0.53	0.76	0.95	1.96		-0.247	0.29	1.67
6	-2.05	-1.75			0.22	0.32	0.57	0.77	2.02		-0.247	0.18	1.84
7		-1.87	-1.38	-0.82	0.57	0.74	1.00		2.10	1.40	-0.333	1.03	1.07
8		-2.06	-1.34	-0.77	0.37	0.60	0.78		2.10	1.14	-0.333	1.29	0.81
9	-1.86	-1.59			0.48	0.72							
10		-1.79		-	0.30	0.62							

Next, computational studies were performed to evaluate the geometry parameters and electronic structures using B3LYP/6-31G* basis set and functional. [49] Figures 4 and S3 show optimized structure, electrostatic potential energy maps and

frontier HOMO-1, HOMO, LUMO and LUMO+1 of investigated compounds while the energies of the frontier orbitals are given in Table S1. Although closely spaced, no steric crowding was witnessed in these systems. In the MP-Donor systems, HOMO was found to be spread on the second donor and part of it on the

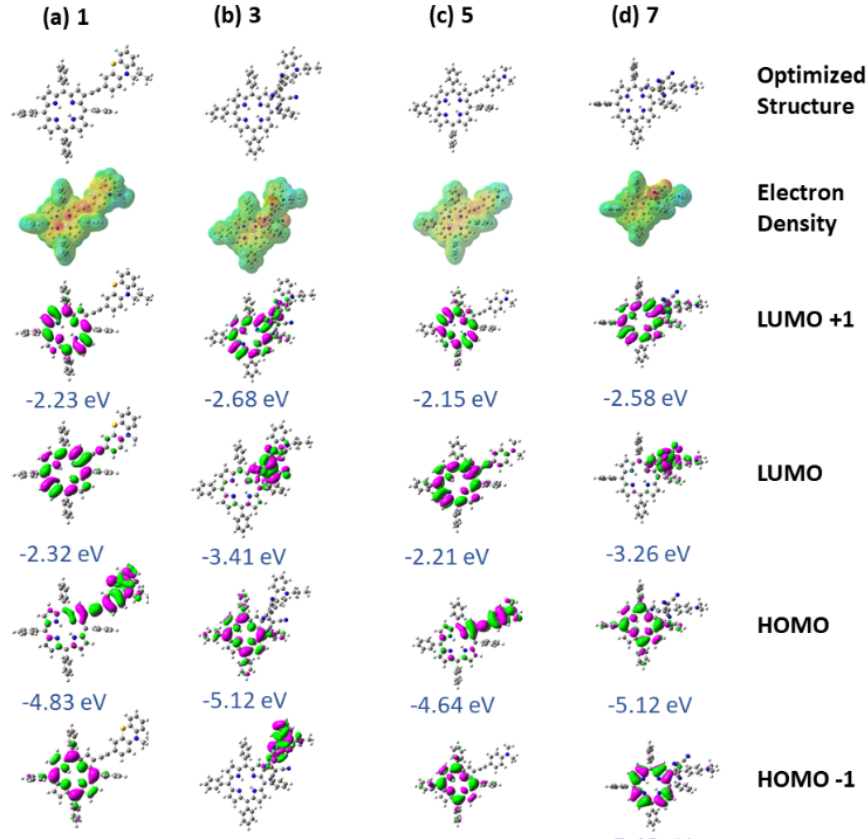
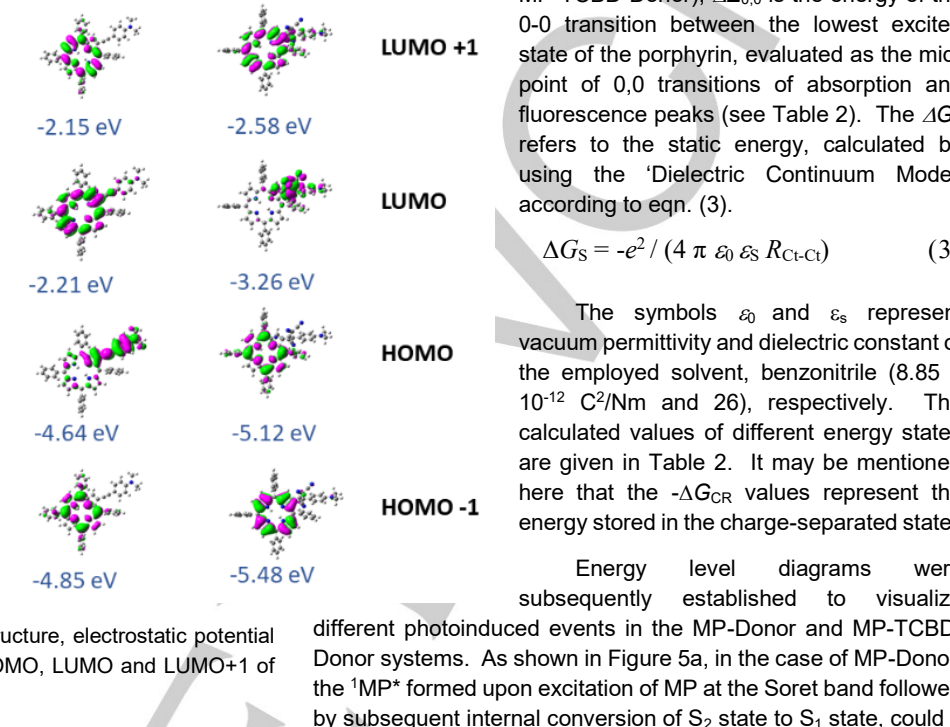


Figure 4. B3LYP/6-31G* optimized structure, electrostatic potential energy maps and frontier HOMO-1, HOMO, LUMO and LUMO+1 of the indicated compounds.

-5.43 eV

porphyrin π -system while LUMO was on the porphyrin ring. These results suggests possibility of MP -- Donor -+ formation during the process of photoinduced electron transfer. Interestingly, in the case of MP-TCBD-Donor systems, a change in the location of HOMO was observed. That is, the HOMO originally located on the second electron donor in the case of MP-Donor systems is moved to the porphyrin π -system, and the LUMO to be mainly on the electron acceptor, TCBD entity. These results suggest formation of MP.+-TCBD:-Donor charge separated state during the process of electron transfer.

-4.97 eV



$$-\Delta G_{\rm CS} = \Delta E_{0,0} - (-\Delta G_{\rm CR})$$
(2)

where E_{ox} is the first oxidation potential of the donor (Donor in the case of MP-Donor and MP in the case MP-TCBD-Donor), Ered is the first reduction potential of acceptor (MP in the case of MP-Donor and TCBD in the case MP-TCBD-Donor), $\Delta E_{0,0}$ is the energy of the 0-0 transition between the lowest excited state of the porphyrin, evaluated as the midpoint of 0,0 transitions of absorption and fluorescence peaks (see Table 2). The ΔG_S refers to the static energy, calculated by using the 'Dielectric Continuum Model' according to eqn. (3).

$$\Delta G_{\rm S} = -e^2 / \left(4 \pi \, \varepsilon_0 \, \varepsilon_{\rm S} \, R_{\rm Ct-Ct} \right) \tag{3}$$

The symbols ε_0 and ε_s represent vacuum permittivity and dielectric constant of the employed solvent, benzonitrile (8.85 x 10⁻¹² C²/Nm and 26), respectively. The calculated values of different energy states are given in Table 2. It may be mentioned here that the $-\Delta G_{CR}$ values represent the energy stored in the charge-separated states.

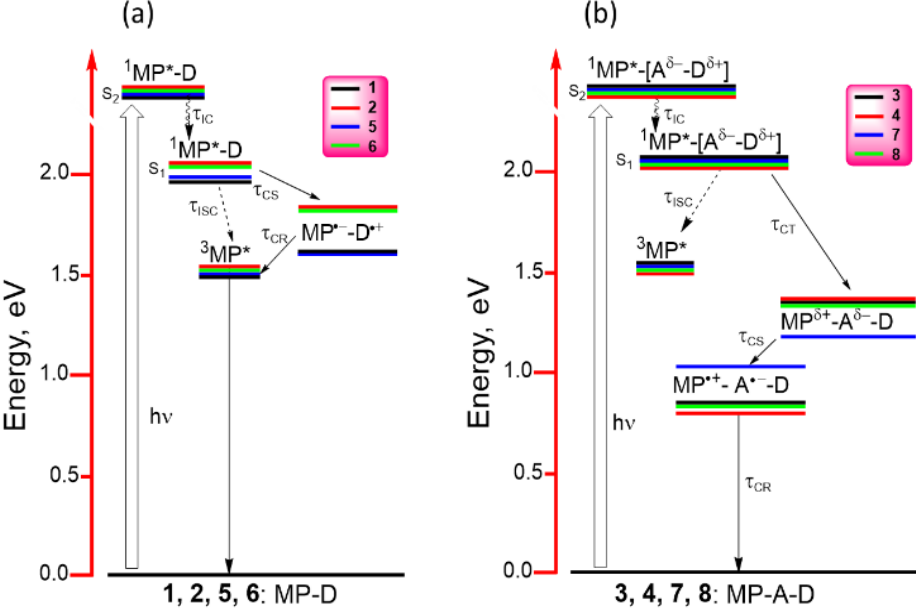
diagrams

were

subsequently established to visualize different photoinduced events in the MP-Donor and MP-TCBD-Donor systems. As shown in Figure 5a, in the case of MP-Donor, the ¹MP* formed upon excitation of MP at the Soret band followed

level

Energy



From the optical, computational and electrochemical data, the driving forces for charge recombination (- ΔG_{CR}) and charge separation (- ΔG_{CS}) were calculated according to egns. (1) and (2) according to Rehm and Weller approach:[50]

$$-\Delta G_{\rm CR} = E_{\rm ox} - E_{\rm red} + \Delta G_{\rm S} \tag{1}$$

Figure 5. Energy level diagrams depicting different photo-events in the (a) MP-D and (b) MP-A-D systems (MP = H_2P or ZnP, A = TCBD, Donor = TPZ or NND). Energy of charge transfer state in Figure 5b is estimated from the charge transfer band shown in Figures 2 and S1.

undergo charge separation to produce MP·-D·+. fluorescence quenching in MP-Donor was in the range of 50-70%, part of ¹MP* could undergo intersystem crossing (ISC) to populate the triplet state, ³MP*. Additionally, since the energy of MP -D + state is higher than that of ³MP*, the charge separated state could also populate ³MP* instead of relaxing directly to the ground state. Interestingly, in the case of MP-TCBD-Donor systems, the ¹MP* formed upon photoexcitation could undergo an initial MP8+-TCBD^δ-Donor charge transfer state. In polar benzonitrile where charge stabilization expected based on earlier discussed energy calculations, the charge transfer state could undergo charge separation process to yield MP.+-TCBD:-Donor. Finally, the charge separated state could relax directly to the ground state. Since the fluorescence quenching was almost quantitative, formation of ³MP* from the initial ¹MP* could be considered negligible. Notably, switching the role of porphyrin from an electron acceptor in MP-Donor systems to an electron donor in MP-TCBD-Donor systems was clear from these energy diagrams.

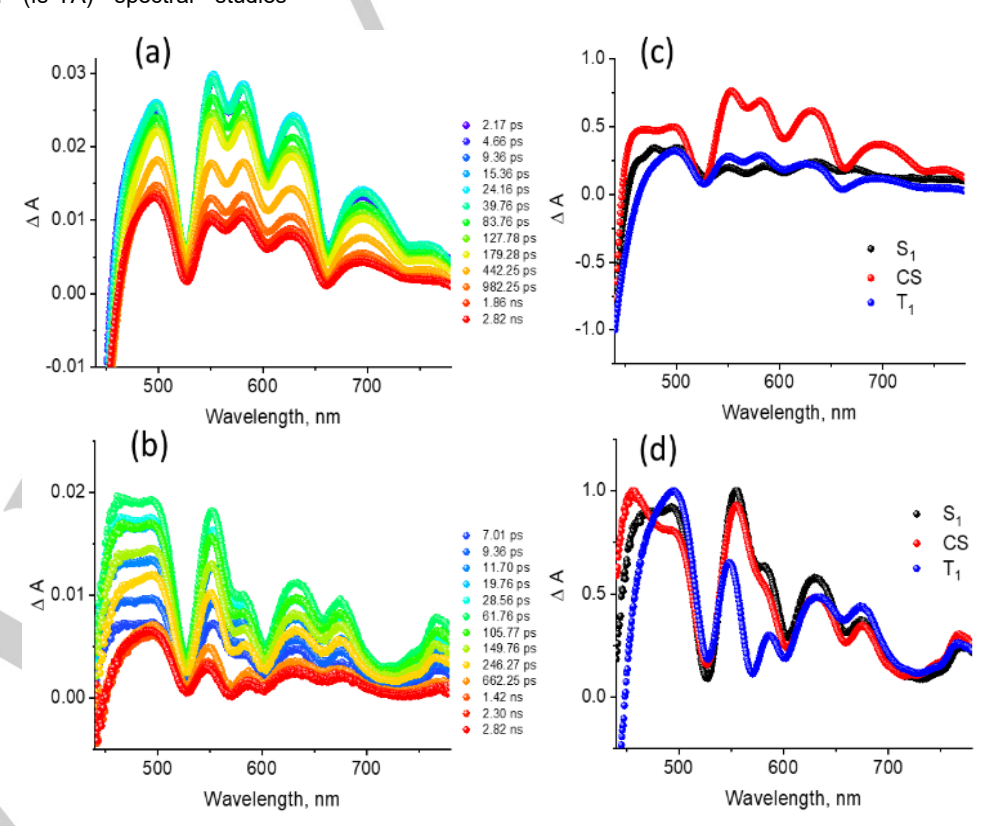
Femtosecond pump-probe studies

To confirm occurrence of charge separation in the MP-Donor and MP-TCBD-Donor systems based on the above discussions, and to evaluate kinetics of such processes, femtosecond transient absorption (fs-TA) spectral studies

followed data analysis using multiwavelength global and target analysis were systematically performed. Among the different entities of the conjugates, the oxidized and reduced species of MP are mainly expected to show signature peaks corresponding to the transient species. Thus, to aid-in spectral identification of such species, spectroelectrochemical studies of control compounds 9 and 10 were performed and are shown in Figure S4. The H_2P^+ (9.+) was characterized by peaks at 445, 463(shoulder peak), 618, and 672 nm while the H₂P⁻⁻ (9⁻⁻) was characterized by peaks at 456, 524, 566, 603 and 656 nm. Similarly, ZnP.+ (10.+) was characterized by peaks at 464 (shoulder peak), 560 and 627 nm, and ZnP- (10-) by peaks at 448, 582 and 625 nm. Most of the peaks corresponding to the radical cation and radical anion were relatively broader compared to their neutral compound analogues.

MP-*. It may be mentioned here that if the Donor entity in MP-TCBD-Donor was involved during first oxidation process then one would expect minimal changes on porphyrin-based absorption peaks.

Figure S6a and S6b show fs-TA at the given delay times of control porphyrins 9 and 10 in benzonitrile. In the case of 9, the instantaneously formed 19* revealed excited state absorption (ESA) peaks at 486, 546, 576, 861, 1102 and 1278 nm. In addition to this, negative peaks at 526, 561, 603, 660 and 728 nm were also observed. By comparison with the earlier discussed absorption and fluorescence spectral results, the first three peaks have been assigned to ground state bleaching (GSB) while part of 660 and the 728 nm have been assigned to stimulated emission (SE). Decay of the positive peaks and recovery of the negative peaks was slow, consistent with long lifetime of 9. In the case of 10, the instantaneously formed 110* had ESA peaks at 480, 586. 633, 842 and 1316 nm, and GSB peaks at 566 and 608 nm, and SE peaks at 608 and 688 nm. Decay/recovery of the positive/negative peaks was accompanied by new peaks at 482 and 856 nm due to subsequent population of 310*. The decay associated spectra (DAS) from Target analysis[51] yielded a lifetime of 10.2 ns for ¹9* (Figure S6c), close to that obtained from the earlier discussed lifetime measurements. Similarly, a lifetime of 1.48 ns was recorded for 110* (Figure S6d) while the lifetime of



Computational calculations predicted HOMO to be on the MP entity in the case of MP-TCBD-Donor systems suggesting MP entity to be the site of electron transfer during first oxidation. To confirm this, spectral changes were monitored during the first oxidation process on all MP-TCBD-Donor systems. As shown in Figure S5, disappearance of neutral porphyrin peaks was accompanied by new peaks corresponding to the formation of

Figure 6. Fs-TA spectra at the indicated delay times of (a) **1** and (b) **5** in benzonitrile (λ_{ex} = 426 nm). Species associated spectra from Target analysis are shown in Figures c and d, respectively, for **1** and **5**.

310* was beyond the time monitoring window. However, reciprocal relationship (decay and growth) of the 856 nm peak confirmed singlet-triplet conversion via the process of intersystem crossing.

Fs-TA spectra of the free-based porphyrin derived dyads 1 and 5 are shown in Figures 6a and 6b while those of zinc porphyrin derived dyads 2 and 6 are shown in Figure S7a and S7b. The earlier discussed energy level diagram predicted

formation of thermodynamically feasible MP -D + charge separated state in the case of both free-base and zinc derived dyads. In the case of 1, the instantaneously formed 11* revealed ESA peaks at 496, 552, 582, 630, 696 and 1076 nm. This was accompanied by negative peaks at 526, 568, 605, 664 and 740 nm (see spectrum at the delay time of 2.16 ps). By comparison with the earlier discussed absorption fluorescence spectra, the first three signals were assigned to GSB and the latter two to SE. Decay/recovery of the positive/negative peaks were faster than that observed for control 1. Since there was a strong spectral overlap between the free-base porphyrin anion radical of 1 (see spectrum Figure 4a for the control 9:-) and ESA peaks of 11*, the initial spectrum of 11* revealed increased intensity in the spectral region owing to the absorption of electron

transfer product. Such was a trend in the case of **5** also. However, in this case the anticipated **5**⁻ peaks at 460 and 558 nm evolved much more strongly providing direct proof for the formation of the charge separated state (see Figure 6b). It may be mentioned here that the spectrum of PTZ⁺ and NND⁺ were out of range of spectral monitoring window, and was also difficult to isolate due to low molar extinction coefficients.

Further analysis of the transient data was performed by target analysis. The data could be fitted to three components. The species associated spectra (SAS) thus generated for these components is shown in Figures 6c and 6d, respectively. Features of the first SAS matched closely that of singlet excited state while SAS of the second components revealed features expected for the charge separated state, viz., clear peak in the 460 nm regions and positive peaks covering the 510-720 nm range was clear. Time constants for this state, signifying the average lifetime of the charge separated state were 221.8 and 219.9 ps, respectively, for 1 and 5. The thirds SAS had features of the triplet excited state with a strong peak in the 490 nm range characteristics of ³H₂P*. This is in accordance with the energy diagram where the energy of the charge separated state was wellabove that of ³H₂P*. Under such circumstances, the charge separated state populating the low-lying triplet state is expected.

Charge separation was also possible to establish in the case of zinc porphyrin derived dyads **2** and **6**, as shown in Figure S7. In the case of both dyads, the instantaneously formed ¹ZnP* revealed faster decay/recovery of the ESA/GSB, SE peaks

compared to its control compound **10** with new transient peaks expected for the ZnP- species thus confirming occurrence of charge separation. The data was further analysed by target analysis (see Figure S7 right hand panel) which gave satisfactory results for the $S_1 \rightarrow CS \rightarrow T_1$ transition. Peak positions for each transient state observed in the SAS nicely matched that expected for the individual states.

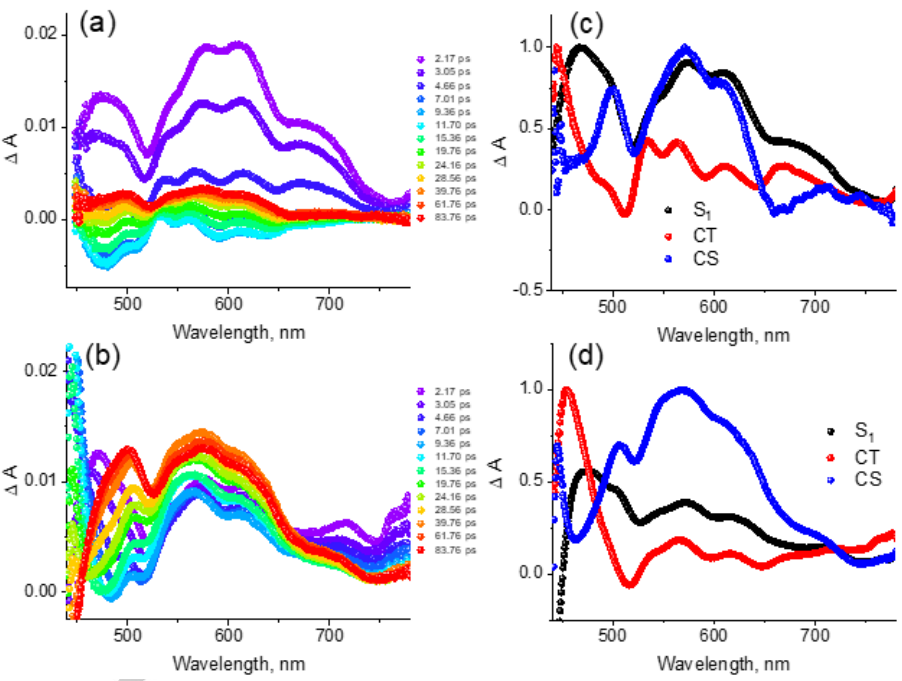


Figure 7. Fs-TA spectra at the indicated delay times of (a) **3** and (b) **7** in benzonitrile (λ_{ex} = 430 nm). Species associated spectra from Target analysis are shown in Figures c and d, respectively, for **3** and **7**.

Having established charge separation in the MP-Donor dyads, next, we focussed out attention on the MP-TCBD-Donor systems. Energy level diagram shown in Figure 5b predicted S₁ → CR → CS transition, that is, sequential formation of ¹MP* → $MP^{\delta+}$ -TCBD $^{\delta-}$ -Donor \rightarrow $MP^{\cdot+}$ -TCBD $^{\cdot-}$ -Donor. Transient data shown in Figure 7 for free-base porphyrin derived compounds 3 and 7, and in Figure S8 for zinc porphyrin derived compounds 4 and 8 were in agreement with the occurrence of the envisioned photo-events. Here, the instantaneously formed ¹MP* revealed the expected ESA, GSB and SE peaks in less than 1 ps transforming into the charge transfer state. Within the next 9-10 ps, the charge transfer state subsequently transformed to the charge separated states, revealing characteristic peaks of MP.+ in the visible region. Interesting, decay of the transient peaks corresponding to the charge separated state did not populate the ³MP* indicating that this state charge recombined directly to the ground state. The SAS spectra from Target analysis (see Figures 7 and S8 right hand panels) were in full agreement with the spectral features expected for the different states.

Table 3 lists time constants for different photo-events (average lifetime of the transient species) for the investigated MP-Donor and MP-TCBD-Donor systems in benzonitrile. Presence of zinc in the porphyrin cavity, and nature of Donor in stabilizing the charge separation are the direct outcomes. Between the free-

base and zinc porphyrin derivatives, charge separated state persisted better in free-base porphyrin derivatives compared to their respective zinc porphyrin analogues. Among the PTZ and NND Donor entities, PTZ seem to have better effect in terms of stabilizing the charge separated states. This could be rationalized based on the energy diagram shown in Figure 5. In the case of MP-Donor, energy of the charge separated states of 2 and 6 are higher than that of 1 and 5. Higher driving force for charge recombination to ³MP* lowered the overall lifetime of the charge separated state. An opposite trend was observed for MP-TCBD-Donor systems, wherein the higher energy of charge separated states in the case of free-base porphyrin derived systems slowed down the charge recombination process to some extent suggesting that this process to belong to the Marcus inverted region. [52]

Table 3. Time constants from Target analysis for the different photoevents of the studied compounds in benzonitrile.

Compound	λ_{ex} , nm	S, ps	CT, ps	CS, ps	T, ns
1	426	0.41		221.79	> 3
2	426	0.99		216.87	> 3
3	429	1.97	10.86	56.12	
4	438	0.90	10.51	40.53	
5	424	0.70		209.94	> 3
6	433	0.46		197.72	> 3
7	430	0.66	9.60	37.63	
8	438	0.50	8.88	31.38	

Conclusions

In conclusion, the MP-Donor and MP-TCBD-Donor systems, functionalized *via* β-pyrrolic positions, revealed several interesting results. These include: (i) the developed synthetic strategy was successful in making directly linked MP-TCBD-Donor systems; (ii) proof for charge transfer interactions was possible to secure from optical studies; (iii) electrochemical and computational studies coupled with energy calculations suggested the formation of MP-Donor·* in the case of MP-Donor, and MP-*-TCBD·-Donor in the case of MP-TCBD-Donor systems, that is, the role of MP was reversed from initial electron acceptor to electron donor; (iv) Fs-TA studies coupled with global and Target analysis unequivocally proved occurrence of charge separation in both MP-Donor and MP-TCBD-Donor systems; (v) finally, the significance of second Donor and metal ion in the porphyrin cavity in stabilizing the charge separated state was borne out from this study.

Conflict of interest

The authors declare no conflict of interest.

Acknowledgements

Support from the Council of Scientific and Industrial Research (Project No. CSIR 01(2934)/18/EMR-II), New Delhi and SERB (Project No. CRG/2018/000032) New Delhi, Govt. of India, and US-National

Science Foundation (2000988 to FD) is gratefully acknowledged. We gratefully acknowledge the Sophisticated Instrumentation Centre (SIC), IIT Indore. B. S. thanks Indian Institute of Technology (IIT), Indore for fellowship.

Keywords: Push-pull, charge transfer, photoinduced charge separation, tetracyanobutadiene, ultrafast spectroscopy.

References and Notes

- Blankenship, R. E. Molecular Mechanisms of Photosynthesis. 2nd Ed. Wiley Blackwell, 2014.
- [2] J. Deisenhofer, O. Epp, K. Miki, R. Huber and H. Michel, Journal of Molecular Biology, 1984, 180, 385–398.
- [3] N. Armaroli and V. Balzani, Angew. Chem. Int. Ed., 2007, 46, 52-66.
- [4] P. M. Beaujuge and J. M. J. Fréchet, J. Am. Chem. Soc., 2011, 133, 20009–20029.
- [5] F. D'Souza and O. Ito, Chem. Soc. Rev., 2012, 41, 86-96.
- [6] M. E. El-Khouly, S. Fukuzumi and F. D'Souza, ChemPhysChem, 2014, 15, 30–47.
- [7] Delgado, J. L.; Bouit, P.-A; Filippone, S.; Herranz, M. A.; Martin, N. Organic Photovoltaics: A Chemical Approach. Chem. Commun. 2010, 46, 4853-4865.
- [8] H. Imahori, T. Umeyama and S. Ito, Acc. Chem. Res., 2009, 42, 1809– 1818.
- [9] D. Gust, T. A. Moore and A. L. Moore, Faraday Discuss., 2012, 155, 9– 26.
- [10] N. Martín, L. Sánchez, M. Á. Herranz, B. Illescas and D. M. Guldi, Acc. Chem. Res., 2007, 40, 1015–1024.
- [11] G. Bottari, G. de la Torre, D. M. Guldi and T. Torres, Chem. Rev., 2010, 110, 6768–6816.
- [12] N. Zarrabi, S. Seetharaman, S. Chaudhuri, N. Holzer, V. S. Batista, A. van der Est, F. D'Souza and P. K. Poddutoori, J. Am. Chem. Soc., 2020, 142, 10008–10024.
- [13] L. Hammarström, Acc. Chem. Res., 2015, 48, 840-850.
- [14] A. Arrigo, A. Santoro, F. Puntoriero, P. P. Lainé and S. Campagna, Coordination Chemistry Reviews, 2015, 304–305, 109–116.
- [15] A. Mishra and P. Bäuerle, Angew. Chem., 2012, 124, 2060-2109.
- [16] M. Gilbert and B. Albinsson, Chem. Soc. Rev., 2015, 44, 845-862.
- [17] K. M. Kadish, K. M. Smith and R. Guilard, Eds., *The porphyrin handbook*, Academic Press, San Diego, Calif., **2000**.
- [18] S. Fukuzumi, T. Honda and T. Kojima, Coordination Chemistry Reviews, 2012, 256, 2488–2502.
- [19] C. B. Kc and F. D'Souza, Coordination Chemistry Reviews, 2016, 322, 104–141.
- [20] Fukuzumi, S.; Kotani, H.; Ohkubo, K.; Ogo, S.; Tkachenko, N. V.; Lemmetyinen. J. Am. Chem. Soc. 2004, 126, 1600-1601.
- [21] G. Bottari, G. de la Torre and T. Torres, Acc. Chem. Res., 2015, 48, 900–910.
- [22] G. Bottari, G. de la Torre, D. M. Guldi and T. Torres, Chem. Rev., 2010, 110, 6768–6816.
- [23] F. D'Souza and O. Ito, Chem. Commun., 2009, 4913.
- [24] S. Kirner, M. Sekita and D. M. Guldi, Adv. Mater., 2014, 26, 1482-1493.
- [25] M. Kivala, C. Boudon, J.-P. Gisselbrecht, P. Seiler, M. Gross and F. Diederich, Angew. Chem. Int. Ed., 2007, 46, 6357–6360.
- [26] A. Gopinath, N. Manivannan, S. Mandal, N. Mathivanan and A. S. Nasar, J. Mater. Chem. B, 2019, 7, 6010–6023.
- [27] T. Michinobu, C. Boudon, J.-P. Gisselbrecht, P. Seiler, B. Frank, N. N. P. Moonen, M. Gross and F. Diederich, Chem. Eur. J., 2006, 12, 1889–1905.
- [28] M. Kivala, C. Boudon, J.-P. Gisselbrecht, P. Seiler, M. Gross and F. Diederich, Angew. Chem. Int. Ed., 2007, 46, 6357–6360.
- [29] T. Michinobu, Chem. Soc. Rev., 2011, 40, 2306.
- [30] T. Shoji, S. Ito, K. Toyota, T. Iwamoto, M. Yasunami and N. Morita, Eur. J. Org. Chem., 2009, 2009, 4307–4315.
- [31] P. Gautam, R. Sharma, R. Misra, M. L. Keshtov, S. A. Kuklin and G. D. Sharma, Chem. Sci., 2017, 8, 2017–2024.
- [32] Y. Patil, R. Misra, R. Singhal and G. D. Sharma, J. Mater. Chem. A, 2017, 5, 13625–13633.

- [33] M. Sekita, B. Ballesteros, F. Diederich, D. M. Guldi, G. Bottari and T. Torres, Angew. Chem., 2016, 128, 5650–5654.
- [34] K. A. Winterfeld, G. Lavarda, J. Guilleme, M. Sekita, D. M. Guldi, T. Torres and G. Bottari, J. Am. Chem. Soc., 2017, 139, 5520–5529.
- [35] K. A. Winterfeld, G. Lavarda, J. Guilleme, D. M. Guldi, T. Torres and G. Bottari, Chem. Sci., 2019, 10, 10997–11005.
- [36] H. Gotfredsen, T. Neumann, F. E. Storm, A. V. Muñoz, M. Jevric, O. Hammerich, K. V. Mikkelsen, M. Freitag, G. Boschloo and M. B. Nielsen, ChemPhotoChem, 2018, 2, 976–985.
- [37] P. Gautam, R. Misra, M. B. Thomas and F. D'Souza, Chem. Eur. J., 2017, 23. 9192–9200.
- [38] R. Sharma, M. B. Thomas, R. Misra and F. D'Souza, Angew. Chem., 2019, 131, 4394–4399.
- [39] Y. Rout, Y. Jang, H. B. Gobeze, R. Misra and F. D'Souza, J. Phys. Chem. C, 2019, 123, 23382–23389.
- [40] M. Poddar, Y. Jang, R. Misra and F. D'Souza, Chem. Eur. J., 2020, 26, 6869–6878.
- [41] F. Tancini, F. Monti, K. Howes, A. Belbakra, A. Listorti, W. B. Schweizer, P. Reutenauer, J.-L. Alonso-Gómez, C. Chiorboli, L. M. Urner, J.-P. Gisselbrecht, C. Boudon, N. Armaroli and F. Diederich, *Chem. Eur. J.*, 2014, 20, 202–216.
- [42] D. Koszelewski, A. Nowak-Król and D. T. Gryko, Chem. Asian J., 2012, 7, 1887–1894.
- [43] Y. Jang, Y. Rout, R. Misra and F. D'Souza, J. Phys. Chem. B, 2021, 125, 4067–4075.
- [44] I. S. Yadav, A. Z. Alsaleh, R. Misra and F. D'Souza, Chem. Sci., 2021, 12, 1109–1120.
- [45] a) D. Pinjari, A. Z. Alsaleh, Y. Patil, R. Misra and F. D'Souza, Angew. Chem., 2020, 132, 23905–23913. b) F. Khan, Y. Jang, Y. Patil, R. Misra, F. D'Souza, Angew. Chem. Int. Ed. 2021, in press. https://doi.org/10.1002/anie.202108293
- [46] G.-Y. Gao, J. V. Ruppel, D. B. Allen, Y. Chen and X. P. Zhang, J. Org. Chem., 2007, 72, 9060–9066.
- [47] M. Yeung, A. C. H. Ng, M. G. B. Drew, E. Vorpagel, E. M. Breitung, R. J. McMahon and D. K. P. Ng, J. Org. Chem., 1998, 63, 7143–7150.
- [48] B. Sekaran, Y. Jang, R. Misra and F. D'Souza, Chem. Eur. J., 2019, 25, 12991–13001.
- [49] M. J. Frisch, G. W. Trucks, H. B. Schlegel, G. E. Scuseria, M. A. Robb, J. R. Cheeseman, G. Scalmani, V. Barone, B. Mennucci, G. A. Petersson, H. Nakatsuji, M. Caricato, X. Li, H. P. Hratchian, A. F. Izmaylov, J. Bloino, G. Zheng, J. L. Sonnenberg, M. Hada, M. Ehara, K. Toyota, R. Fukuda, J. Hasegawa, M. Ishida, T. Nakajima, Y. Honda, O. Kitao, H. Nakai, T. Vreven, J. A. Montgomery Jr., J. E. Peralta, F. Ogliaro, M. Bearpark, J. J. Heyd, E. Brothers, K. N. Kudin, V. N. Staroverov, R. Kobayashi, J. Normand, K. Raghavachari, A. Rendell, J. C. Burant, S. S. Iyengar, J. Tomasi, M. Cossi, N. Rega, N. J. Millam, M. Klene, J. E. Knox, J. B. Cross, V. Bakken, C. Adamo, J. Jaramillo, R. Gomperts, R. E. Stratmann, O. Yazyev, A. J. Austin, R. Cammi, C. Pomelli, J. W. Ochterski, R. L. Martin, K. Morokuma, V. G. Zakrzewski, G. A. Voth, P. Salvador, J. Dannenberg, S. Dapprich, A. D. Daniels, O. Farkas, J. B. Foresman, J. V. Ortiz, J. Cioslowski and D. J. Fox, Gaussian 09, revision A.02, Gaussian, Inc., Wallinoford, CT. 2009:
- [50] D. Rehm and A. Weller, Isr. J. Chem., 1970, 8, 259-271.
- [51] J. J. Snellenburg, S. P. Laptenok, R. Seger, K. M. Mullen and I. H. M. van Stokkum, J. Stat. Soft. 2012, 49
- [52] R. A. Marcus and N. Sutin, Biochimica et Biophysica Acta (BBA) Reviews on Bioenergetics, 1985, 811, 265–322.
- [53] P. G. Seybold, M. Gouterman, J. Mol. Spectrosc., 1969, 31, 1-13.



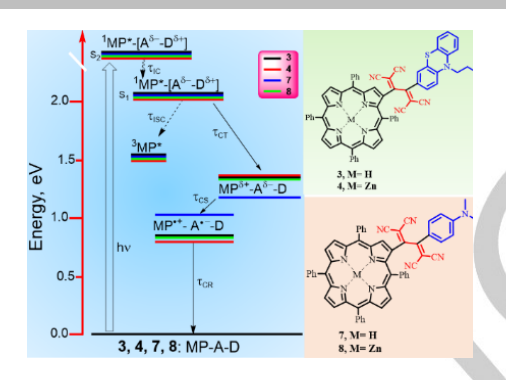
Entry for the Table of Contents

Charge Transfer and Separation

B. Sekaran, A. Dawson, Y. Jang, K. V. MohanSingh, R. Misra* F. D'Souza*

Page No. - Page No.

Charge-Transfer in Panchromatic Porphyrin-Tetracyanobuta-1,3diene-Donor Conjugates: Switching the Role of Porphyrin in the Charge Separation Process



Occurrence of charge transfer and separation processes in newly synthesized porphyrin-TCBD-Donor multi-modular donor-acceptor systems is reported. The significance of the nature of porphyrins and second electron donor in governing the charge transfer events in these closely positioned conjugates is borne out from the present study.

Twitter accounts:

- @UNTChemistry
- @ChemistryIITI

